RESEARCH

Response of cross-correlations between high $PM_{2.5}$ and O_3 with increasing time scales to the COVID-19: different trends in BTH and PRD

**Bingyi Bao · Youping Li · Chunqiong Liu ·
Ye Wen · Kai Shi**

Abstract The air pollution in China currently is characterized by high fine particulate matter ($PM_{2.5}$) and ozone (O_3) concentrations. Compared with single high pollution events, such double high pollution (DHP) events (both $PM_{2.5}$ and O_3 are above the National Ambient Air Quality Standards (NAAQS)) pose a greater threat to public health and environment. In 2020, the outbreak of COVID-19 provided a special time window to further understand the cross-correlation between $PM_{2.5}$ and O_3. Based on this background, a novel detrended cross-correlation analysis (DCCA) based on maximum time series of variable time scales (VM-DCCA) method is established in this paper to compare the cross-correlation between high $PM_{2.5}$ and O_3 in Beijing-Tianjin-Heibei (BTH) and Pearl River Delta (PRD). At first, the results show that $PM_{2.5}$ decreased while O_3 increased in most cities due to the effect of COVID-19, and the increase in O_3 is more significant in PRD than in BTH. Secondly, through DCCA, the results show that the $PM_{2.5}$-O_3 DCCA exponents α decrease by an average of 4.40% and 2.35% in BTH and PRD respectively during COVID-19 period compared with non-COVID-19 period. Further, through VM-DCCA, the results show that the $PM_{2.5}$-O_3 VM-DCCA exponents α_{VM} in PRD weaken rapidly with the increase of time scales, with decline range of about 23.53% and 22.90% during the non-COVID-19 period and COVID-19 period respectively at 28-h time scale. BTH is completely different. Without significant tendency, its α_{VM} is always higher than that in PRD at different time scales. Finally, we explain the above results with the self-organized criticality (SOC) theory. The impact of meteorological conditions and atmospheric oxidation capacity (AOC) variation during the COVID-19 period on SOC state are further discussed. The results show that the characteristics of cross-correlation between high $PM_{2.5}$ and O_3 are the manifestation of the SOC theory of atmospheric system. Relevant conclusions are important for the establishment of regionally targeted $PM_{2.5}$-O_3 DHP coordinated control strategies.

Keywords $PM_{2.5}$-O_3 DHP · Time scale · VM-DCCA · Long-term persistence · SOC

The authors Chunqiong Liu and Kai Shi contributed equally to this work.

B. Bao · Y. Wen
College of Mathematics and Statistics, Jishou University, Jishou, Hunan, China
e-mail: 1834185217@qq.com

Y. Wen
e-mail: wenye.work@qq.com

Y. Li · C. Liu (✉) · K. Shi (✉)
College of Environmental Science and Engineering, China West Normal University, Nanchong, Sichuan, China
e-mail: liuchunqiong@cwnu.edu.cn

K. Shi
e-mail: shikai@cwnu.edu.cn

Y. Li
e-mail: lyp920@163.com

Introduction

Despite the pollutant emissions that have been witnessed significant reduction in recent years, there are still heavy fine particulate matter ($PM_{2.5}$) and ozone (O_3) pollution events in some regions of China (Chen et al., 2022; Qin et al., 2021). Qin et al. (2021) reported that the occurrence of $PM_{2.5}$-O_3 double high pollution (DHP) events in China's major city clusters were driven by a combination of the emissions of pollution sources and regional meteorological factors. It clearly implies that an enhanced understanding of the cross-correlation between high $PM_{2.5}$ and O_3 in a city area has a primary significance to formulating regional targeted $PM_{2.5}$-O_3 DHP coordinated control strategies.

$PM_{2.5}$ and O_3 not only have common precursors nitrogen dioxides (NOx) and volatile organic compounds (VOCs), but also interact with each other through a variety of atmospheric photochemical pathways, causing extremely complex non-linear responses (Chen et al., 2019a; Ding et al., 2013; Liu et al., 2023; Wu et al., 2021b). Firstly, $PM_{2.5}$ can influence the formation and thickness of cloud by acting as a cloud condensation nuclei and enhance atmospheric extinction capacity to alter the photolysis rate, thus indirectly affect the formation of O_3. For instance, Zhu et al. (2019) discovered the strong negative correlation between $PM_{2.5}$ and O_3 in northern China in winter, due to the influence of $PM_{2.5}$ on photolysis rate. Chu et al. (2020) also reported that the increase in actinic flux owing to the reduction of air particles, leads to the rising of O_3 levels in China. Secondly, O_3 can enhance the atmospheric oxidation capacity and thus produce photochemical oxidants such as hydroxyl ($\cdot$OH) radicals, hydrogen peroxide (H_2O_2) and aldehyde (R-CHO). These oxidants can result in the rapid nucleation of secondary aerosol particles and boost the explosive growth of $PM_{2.5}$. For instance, Jia et al. (2017) analyzed the interaction between $PM_{2.5}$ and O_3 in Nanjing in different seasons and found that high O_3 levels in hot season could accelerate the formation of secondary particles. Fu et al. (2020) revealed that atmospheric oxidizing capacity enhanced by high O_3 levels, played a key role in the conversion efficiency of NOx into nitrate (the main component of $PM_{2.5}$ in North China Plain). At last, some other studies highlighted that the heterogeneous reactions of chemicals on particle surface also affect the formation and consumption of O_3 (Qu et al., 2018; Xu et al., 2012). Thus, the complexity of the interaction mechanism between $PM_{2.5}$ and O_3 and the effectiveness of $PM_{2.5}$-O_3 DHP coordinated control in city clusters are closely linked.

Due to the temporal variability of meteorology and pollution emissions, the time scale dependence can be observed in the dominant mechanism of the cross-correlation between $PM_{2.5}$ and O_3. The photochemical mechanism by which photochemical oxidants such as O_3 contribute to the rapid nucleation of secondary aerosol particles occurs mainly on the time scale of seconds to hours. For example, Wang et al. (2014) found that the explosive growth of $PM_{2.5}$ levels in Beijing-Tianjin-Heibei mainly occurred at the time scale of several hours. At the same time, the photochemical mechanism by which particulate matter affects O_3 formation by scattering solar radiation occurs on daily, weekly, monthly and even longer time scales. For example, Xing et al. (2017) studied the impact of aerosol direct effects (ADEs) on tropospheric O_3 in China and found that ADEs led to a decrease in the average O_3 concentrations at time scale up to 1 month. In addition, the correlation between $PM_{2.5}$ and O_3 is also affected by the selection of research period. For example, Zhao et al. (2018) pointed out that the $PM_{2.5}$ was positively correlated with the daily maximum of O_3 at a 3-month scale in summer (from June to August 2016) and negatively correlated with it at a 3-month scale in winter (from December 2016 to February 2017). Conversely, Chou et al. (2011) discovered an inverse correlation between $PM_{2.5}$ and O_3 at the time scale of nearly 1 month during the Beijing Olympic Games in August 2008. During the city-lockdown period from January 23 to February 13, 2020 in northern China, a positive correlation between O_3 and $PM_{2.5}$ at the time scale of 22 days was observed by Le et al. (2020). These ambiguous conclusions, which show both positive and inverse correlation between $PM_{2.5}$ and O_3, are largely related to the sampling periods. Finally, several studies have showed that the correlation between $PM_{2.5}$ and O_3 is also affected by meteorological factors (Chen et al., 2019b; Liu & Shi, 2021). For example, Chen et al. (2017) showed that the correlation coefficients of O_3 and five other conventional pollutants (including $PM_{2.5}$) were less than 0.4 in warm seasons, while they were weak or negatively correlated in cold seasons. Therefore, it is essential to

investigate the differences in the correlation between $PM_{2.5}$ and O_3 and evolution over time scales in different climate zones.

It is generally believed that the differences in regional pollution emission will interfere with the assessment of the impact of meteorology on air pollution. In 2020, with the outbreak of the COVID-19, the Chinese government adopted a series of nationwide compulsory measures such as city closure, travel restriction and plant shutdown to control the spread of the epidemic. As a result, primary pollutants were greatly reduced, which led to a similar initial atmospheric condition in different regions (Bherwani et al., 2021; Gautam, 2020; Gautam et al., 2021). Kumar et al. (2022) compared the air pollutant levels during the Christmas and New Year celebration in 2019, 2020 and 2021 and found lower total concentration of air pollutants than the previous year when there was no pandemic situation in India. Such confinement served as a natural experiment for scholars to accurately evaluate the impacts on the formation of regional pollution. For example, Chelani and Gautam (2022) studied the correlation between $PM_{2.5}$ and NO_2 concentrations and indicated that the inherent temporal characteristics of the short-term air pollutant concentrations (APCs) time series do not change even after withholding the emissions. However, current studies have mainly considered the variations in pollutant concentrations during COVID-19. The cross-correlation between secondary pollutants $PM_{2.5}$ and O_3 has rarely been studied.

Due to the non-linearity and complexity of evolution of secondary pollutants, existing atmospheric chemistry models are hard to meet the requests of high accuracy for research data and may result in deviations in the simulation of air quality under extreme conditions (Liu et al., 2020). In order to eliminate the misleading or non-robust effects caused by non-stationarity of nonlinear series, Peng et al. (1995) first proposed detrended fluctuation analysis (DFA), which is suitable for investigating the long-term autocorrelation of non-stationary time series. Further, Podobnik and Stanley (2008) proposed a detrended cross-correlation analysis (DCCA) method suitable for studying the long-term persistence of cross-correlations between two non-stationary time series. This method can effectively avoid the pseudo-correlation between the series due to non-stationary data, and analyze the time scale characteristics of the interaction between two groups. DCCA has been efficiently

applied in the analysis of the interaction between pollutants at multiple time scales. For example, Shi (2014) used the DCCA method to reveal that the relationship between ambient dioxins and precipitation (or PM_{10}) manifested a long-term cross-correlation at the time scale ranging from 1 month to 1 year. Du et al. (2021) applied DCCA method to report that the high-frequency mode of NO_2 between urban area and scenic spots in Zhangjiajie at different time scales showed long-term cross-correlation at 24-h time scale. He (2016) used DCCA method to find that there was a long-term cross-correlation between pollutants and meteorology at a 10-year time scale, and it was more obvious in rural areas. DCCA method has been widely used in some other fields (Chen et al., 2018a; Liang et al., 2017; Rohit & Mitra, 2018; Yuan & Fu, 2014), and its scientificity and applicability have been proved by many scholars.

Taking Beijing-Tianjin-Heibei (BTH) and Pearl River Delta (PRD) as the study areas, this study establishes a new VM-DCCA method based on DCCA method to extract high pollutants, thus to compare time scale characteristics of the cross-correlation between high $PM_{2.5}$ and O_3. The primary objective is to consider the spatiotemporal evolution of the interaction between these two pollutants and attempt to provide a quantitative basis of devising sustainable coordinated control strategies of high $PM_{2.5}$ and O_3 in city clusters in different climate zones.

Materials and methods

Study areas

Both the Beijing-Tianjin-Hebei (BTH) and the Pearl River Delta (PRD) are the major city clusters in China. The BTH (39°28′N-41°05′N, 115°20′E-117°30′E) is located in the north of North China Plain, including two municipalities (Beijing and Tianjin) and 11 prefecture level cities (Baoding, Tangshan, Langfang, Shijiazhuang, Qinhuangdao, Handan, Zhangjiakou, Chengde, Cangzhou, Xingtai and Hengshui). This region belongs to temperate continental monsoon climate, with high temperature and rainy in summer due to the impact of the ocean water vapor and cold and dry in winter due to the impact of the cold inland air (Sun et al., 2021). The PRD (21°31′N-23°10′N, 112°45′E-113°50′E) is located in

the south central part of Guangdong Province, China, including 9 cities (Dongguan, Foshan, Guangzhou, Huizhou, Jiangmen, Shenzhen, Zhaoqing, Zhongshan and Zhuhai). This region belongs to subtropical monsoon climate, with abundant rainfall and heat throughout the year. The rain and heat are in the same season, and the four seasons are relatively evenly distributed (Li et al., 2018). The total GDP of BTH and PRD were 8.69 and 8.95 trillion, accounting for about 8.54% and 8.77% of the national GDP respectively by 2020. There are a large number of advanced manufacturing bases and factories with global influence and developed industries in the two regions, which lead to intensive energy consumption and pollutant emission in the two regions, bringing serious atmospheric pollution to the local (Chen et al., 2018b; Hu et al., 2021).

Data source

According to the National Emergency Response Plan for Public Health Emergencies, control measures were implemented throughout the country on around January 24, 2020, and all work and production activities resumed in early May. In this study, January 24 to May 31, 2020 are set as the COVID-19 period and the same period in 2019 is set as the non-COVID-19 period for comparison. Hourly observations of $PM_{2.5}$ and O_3 are obtained from the China National Environmental Monitoring Centre (http://www.cnemc.cn/). Due to instrument calibration, power failure and some other factors, it is inevitable to cause the lack of individual data, accounting about 0.1%. These lacking data have been replaced by the average of the two adjacent data. Besides, daily meteorological data including minimum temperature (T-Min), maximum temperature (T-Max), precipitation (Pre), relative humidity (HR), wind speed (WS) and atmospheric pressure (P) are obtained from the China Meteorological Administration (http://cma.gjzwfw.gov.cn/). The statistical analyses of these meteorological factors are shown in Fig. 1 (For each box, the upper and lower boundaries of the box represent the 75th and 25th percentile respectively, the horizontal line in the box represents the median, the beard represents the minimum and maximum respectively, and the square represents the average, which has been marked). According to Fig. 1, there are no significant differences between

Fig. 1 The statistics of meteorological factors during the non-COVID-19 period and COVID-19 period in BTH and PRD
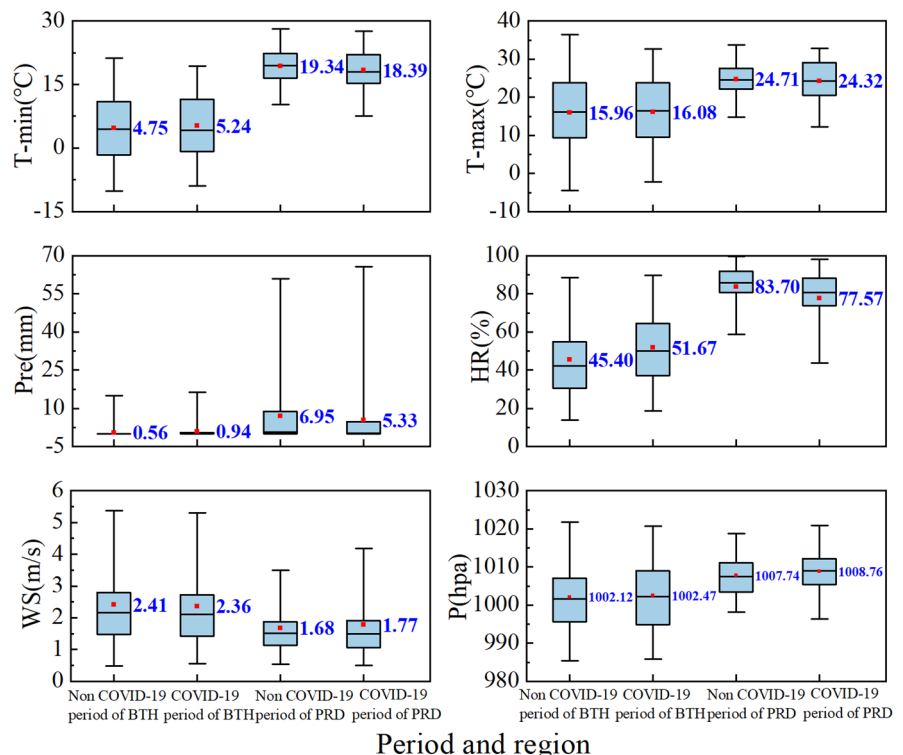
BTH and PRD in WS and P, while the other four meteorological factors are completely different. During the non-COVID-19 period, the T-min, T-max, Pre and HR in PRD are about 14.59℃, 8.75℃, 6.39 mm, 38.3% higher than BTH respectively, and about 13.15℃, 8.24℃, 4.39 mm, 25.9% higher respectively during the COVID-19 period. In this way, the great differences in meteorological factors between the BTH and PRD are conducive to the comparative analysis of the impacts of different meteorological factors on compound atmospheric pollution.

Methods

Detrended cross-correlation analysis based on maximum time series of variable time scales

Compared with traditional method for correlation analysis, the advantage of DCCA related methods is that the scales characteristic of correlations can be quantified. Piao and Fu (2016) compared the Pearson method with DCCA method and reported that DCCA related methods can quantify scale-dependent correlations and are robust to contaminated noises and amplitude ratio, but not Pearson method. The calculation process is as follows.

Firstly, the series $\{x_k\}$ and $\{y_k\}$ are calculated as follows:

$$x_k = \sum_{t=1}^{k} \left(x_t - \bar{x}\right) \text{ and } y_k = \sum_{t=1}^{k} \left(y_t - \bar{y}\right), \; k = 1, 2, \cdots, S \tag{1}$$

where $\{x_t, t = 1, 2, \cdots, S\}$ and $\{y_t, t = 1, 2, \cdots, S\}$ are the original time series, $\bar{x}$ and $\bar{y}$ are the averages of them, respectively.

Secondly, the above series $\{x_k\}$ and $\{y_k\}$ are divided into equal segments with length s (s represents the length of time scale), the least square method is used for linear fitting of each segment, thus, the local trend of data fluctuation at a specific time scale s is obtained. Then the trend of each data segment is combined as local trend $x_{k,t}$, $y_{k,t}$.

Thirdly, the trend signal is subtracted from the cumulative signal to obtain the residual signal, and the covariance of each residual signal is calculated as follows:

$$f_{DCCA}^2(s,t) = \frac{1}{s-1} \sum_{k=t}^{t+s} (x_t - \tilde{x}_{k,t})(y_t - \tilde{y}_{k,t}) \tag{2}$$

The covariance of the whole time series is

$$F(s) \equiv \sqrt{\sum_{t=1}^{N-n} \left[\frac{1}{s-1} \sum_{k=t}^{t+s} (x_k - \tilde{x}_{k,t})(y_k - \tilde{y}_{k,t})\right]} \tag{3}$$

Finally, repeat the above steps for each time scale s to obtain logarithmic relationship curves of $F(s)$ and s. If $\ln s \sim \ln F(s)$ satisfy a linear relationship, a power-law relationship $F(s) \propto s^\alpha$ exists. A linear fit is performed at this point, and the slope is the DCCA exponent α.

For a specific time scale, α quantitatively represents the cross-correlation between the two groups of non-stationary time series. $\alpha > 0.5$ represents that there is a lasting positive cross-correlation in a power-law form between the two groups of time series, that is, there is a trend of increase (or decrease) in a group of time series that will be followed by the same trend in the other group of time series at a certain time scale. The larger the α, the stronger the positive cross-correlation between the two groups of time series. $\alpha < 0.5$ indicates that there is a continuous negative cross-correlation between the two groups of non-stationary time series variables, and the specific meaning is opposite to that when $\alpha > 0.5$. $\alpha = 0.5$ indicates that there is no cross-correlation between the two groups of time series.

Due to the adverse effects of extreme pollution (Kumar et al., 2023), the correlation between high $PM_{2.5}$ and O_3 should be further explored. The formation of high pollution strongly relies on the time scale, but the traditional DCCA method cannot identify the correlation between high pollutants at different time scales. So the simultaneous series of high $PM_{2.5}$ and O_3 at different time scales should be obtained first.

This paper applies the method proposed by Muchnik et al. (2009) to obtain the series of high pollutants. Specifically, Fig. 2a shows typical hourly average concentrations series of $PM_{2.5}$ and O_3 for 48 sequential hours. They are divided into several segments with interval length of 4 h, and the maxima of each interval are marked. Thus, Fig. 2b represents the maximum sequences of $PM_{2.5}$ and O_3 at a 4-h interval. Similarly, by changing the length of the period,
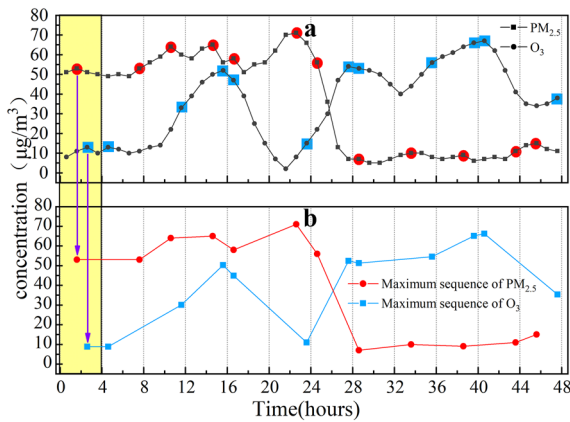
Fig. 2 Maximum sequences of $PM_{2.5}$ and O_3 obtained from original sequence with interval length of 4 h

maximum sequences of $PM_{2.5}$ and O_3 at different interval length can be obtained. At last, the VM-DCCA exponent α_{VM} can be further obtained by the same steps of DCCA, and the meaning of α_{VM} is similar to α. α_{VM} varies with the interval length, which reflects the cross-correlation between high $PM_{2.5}$ and O_3 at different time scales.

Self-organized criticality

Self-organized criticality (SOC) theory was proposed by Bak et al. (1987), which explained the dynamic mechanism of the power-law distribution characteristics of complex systems. In general, a complex system consists of many cells that have short-term correlation. Under certain conditions, the system spontaneously evolves and reaches the critical state. At this state, a slight perturbation would lead to large-scale

events through spatial association between each cell, and the "frequency-size" distribution of these events obeys a power-law relation.

The "sandpile model" is used to illustrate the physical significance of SOC theory. Individual grains are dropped and gradually form a small pile, and then simulate and calculate how many grains will slide when a grain falls. In the initial stage, the falling grains just add to the growing pile, but as the grains accumulate to a certain extent, it stops growing and reaches a critical slope in a statistically stationary state. At this moment, the result of adding grains is unpredictable. The addition of grains may cause either a small perturbation or even trigger a large avalanche. Statistical analysis suggests that the frequency of avalanches is a power-law function with the size of the pile in the long-term grain adding process.

Results

Concentrations variations of $PM_{2.5}$ and O_3 during the COVID-19 period

Figure 3 shows the variations of $PM_{2.5}$ and O_3 during the COVID-19 period compared with the non-COVID-19 period. For BTH, $PM_{2.5}$ in most cities shows a downward trend, ranging from 4.72 to 32.34%, and shows a slight increase in a small number of cities. By contrast, O_3 in most cities shows an upward trend, ranging from 1.25 to 6.36%, and declines slightly in a small number of cities. For PRD, $PM_{2.5}$ in all cities decreases significantly, ranging from 7.78 to 32.44%. Except Shenzhen, O_3 in other cities shows an upward trend, ranging

Fig. 3 Variations of $PM_{2.5}$ and O_3 in each cities of BTH and PRD during the COVID-19 period compared with the non COVID-19 period
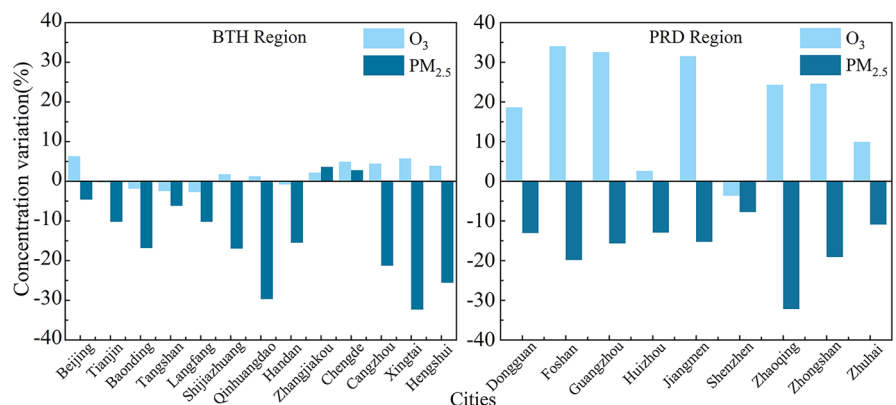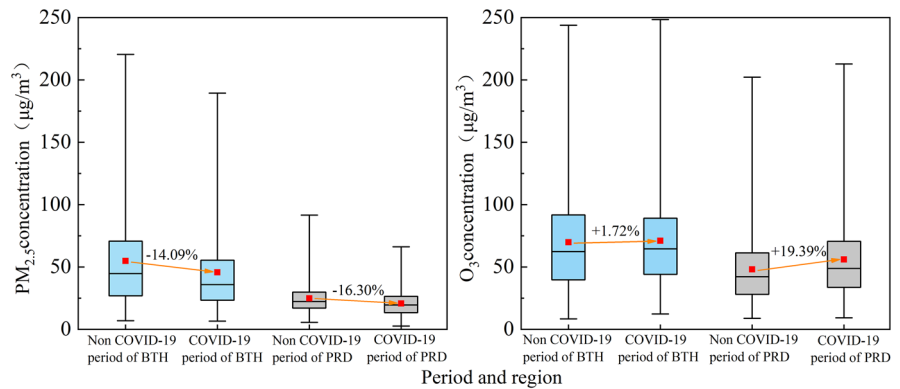
Fig. 4 Averaged variations of $PM_{2.5}$ and O_3 in BTH and PRD during the COVID-19 period compared with the non-COVID-19 period

from 2.60 to 33.99%. This result shows that $PM_{2.5}$ decreased while O_3 increased in most cities due to the impact of COVID-19. The rise in O_3 is not only related to the decrease in $PM_{2.5}$, but is also influenced by the decrease in the concentration of its precursors NOx, which reduced the titration of O_3.

Figure 4 shows the comparison of variances above of $PM_{2.5}$ and O_3 in BTH and PRD. In general, there is no significant difference in concentrations variations of $PM_{2.5}$ between BTH and the PRD. $PM_{2.5}$ decreases by 14.09% and 16.30% in BTH and PRD respectively. Comparatively, the increment of O_3 in PRD is much higher than that in BTH. The average O_3 concentrations increase by 1.72% in BTH, but 19.39% in PRD. This result suggests that there is obvious regional difference in the responses of $PM_{2.5}$ and O_3 to the reduction of primary emission. The increase of O_3 in the PRD is much larger than that in BTH, which may be influenced by meteorological differences between two regions.

Long-term cross-correlation between $PM_{2.5}$ and O_3 during the COVID-19 period

In order to explore the long-term cross-correlation between $PM_{2.5}$ and O_3 in BTH and PRD, taking Beijing and Guangzhou as examples, the DCCA result during the COVID-19 period is shown in Fig. 5. As shown in the figure, there is a linear relationship between the covariance fluctuation function $F(s)$ and time scales s with logarithm. The α values are 0.84 and 0.89 in Beijing and Guangzhou respectively, indicating that the cross-correlation between $PM_{2.5}$ and O_3 during the COVID-19 period shows strong long-term persistence characteristics.

In order to verify whether DCCA method truly reflects the long-term persistence characteristics of the cross-correlation between non-stationary series, this paper applies the same way to analyze the random shuffled series. According to Markov process theory, if the time series x_i and y_i of the two pollutants

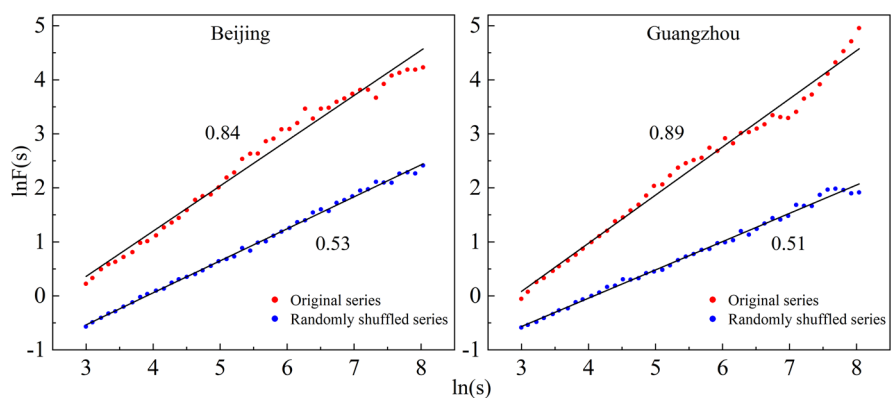**Fig. 5** DCCA plot of $PM_{2.5}$ and O_3 in Beijing and Guangzhou during the COVID-19 period

Table 1 The main statistical values of DCCA exponents α during COVID-19 period and non-COVID-19 period in BTH and PRD

| City clusters		Mean value ($\mu g/m^3$)	Standard deviation	Skewness	Kurtosis	Shapiro–Wilk test	T test
BTH	Non-COVID-19 period	0.91	0.06	−0.12	1.53	Obey normal distribution	Exist
	COVID-19 period	0.87	0.02	0.12	1.91	Obey normal distribution	significant differences
PRD	Non-COVID-19 period	0.85	0.02	0.74	2.51	Obey normal distribution	Exist significant differences
	COVID-19 period	0.83	0.03	−0.68	2.24	Obey normal distribution	

are completely random, the correlation function will decay exponentially with time, and the correlation coefficient is 0 at a specific time. In this paper, the original $PM_{2.5}$ and O_3 are randomly shuffled and then analyzed by DCCA, which show an obvious power-law relationship of the two cities at the whole time scale, and its α values are 0.53 and 0.51 respectively, which indicate that there is no correlation between the randomly shuffled series. The comparative result shows that DCCA method can effectively reveal the long-term persistence of the cross-correlation between original $PM_{2.5}$ and O_3 series at a long time scale.

Based on the above analyses, DCCA calculation of $PM_{2.5}$ and O_3 concentration series during COVID-19 and non-COVID-19 period in BTH and PRD is further carried out. It can be seen from Fig. 5 that the α values of BTH and PRD fluctuate between 0.78 and 0.99, which means the correlation between $PM_{2.5}$ and O_3 series in each city shows strong long-term persistence. Besides, the α values during the COVID-19 period is lower than that during the non-COVID-19 period in most cities. Table 1 shows the statistical

analysis of α values during the COVID-19 and non-COVID-19 period in the two regions.

The Shapiro–Wilk test is performed to test the normality of α values series. The results show that the α values obey the normal distribution. The T-test is used to compare the difference of α values between the two periods, which show that the P values of BTH and PRD are 0.02 and 0.02 respectively, which are less than the set significance level (0.05). Therefore, the null hypothesis that there is no significant difference in α values between the COVID-19 and non-COVID-19 period is rejected, that is, the α values are significantly different during the two periods. As shown in Fig. 6, the α values of most cities during the COVID-19 period decrease significantly compared with that in the non-COVID-19 period. The average α values are 0.91 and 0.85 respectively in BTH (decreasing by 4.40%), while are 0.87 and 0.83 respectively in PRD (decreasing by 2.35%). The results indicate that the long-term persistence of $PM_{2.5}$-O_3 correlation has weakened during the COVID-19 period in both regions.

Fig. 6 Comparison of DCCA exponents α of $PM_{2.5}$ and O_3 between COVID-19 period and non-COVID-19 period in each cities of BTH and PRD
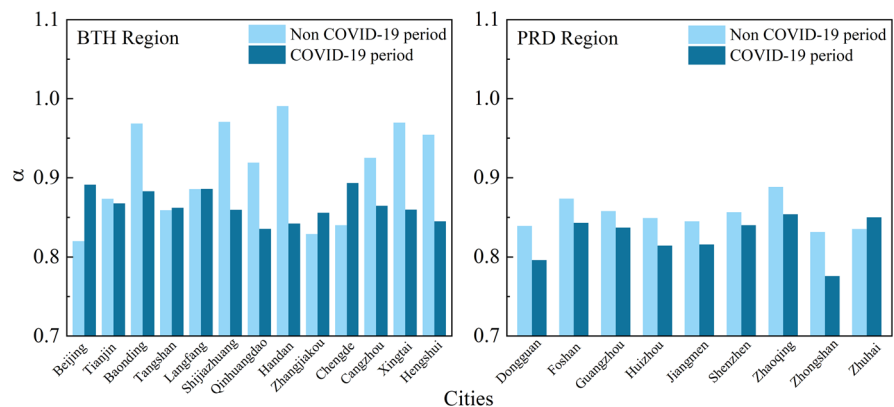
Long-term cross-correlation between high PM$_{2.5}$ and O$_3$ concentrations

The spatiotemporal distribution of PM$_{2.5}$ or O$_3$ high pollution events, in which the daily average concentration of PM$_{2.5}$ is above 75 $\mu g/m^3$, and the daily maximum 8-h average ozone (MDA8 O$_3$) concentration is above 160 $\mu g/m^3$, in BTH and PRD during the non-COVID-19 period and COVID-19 period are compared at first. As is shown in Fig. 7, the frequency of high pollution events in BTH is higher than that in PRD. Specifically, for PM$_{2.5}$, the frequency of high pollution events is higher during the non-COVID-19 period. For O$_3$, the frequency of high pollution events is higher during the COVID-19 period.

Further, taking 1 h (original concentration series), 4 h, 8 h, 12 h, 16 h, 20 h, 24 h and 28 h as interval length, the cross-correlation between high PM$_{2.5}$ and O$_3$ is analyzed by VM-DCCA method. Its VM-DCCA exponents α_{VM} varying with the intervals are shown in Fig. 8.

It can be seen from Fig. 8 that α_{VM} values during the non-COVID-19 period are always higher than that during the COVID-19 period at different interval length both in BTH and PRD. It indicates that the long-term cross-correlation between high PM$_{2.5}$ and O$_3$ during the COVID-19 period is weaker than that in the non-COVID-19 period. Secondly, the α_{VM} values in BTH are always higher than that in PRD, which illustrates that the long-term cross-correlation between high PM$_{2.5}$ and O$_3$ in BTH is stronger than that in PRD. Moreover, with the increase of interval length, α_{VM} values in BTH fluctuate between 0.91
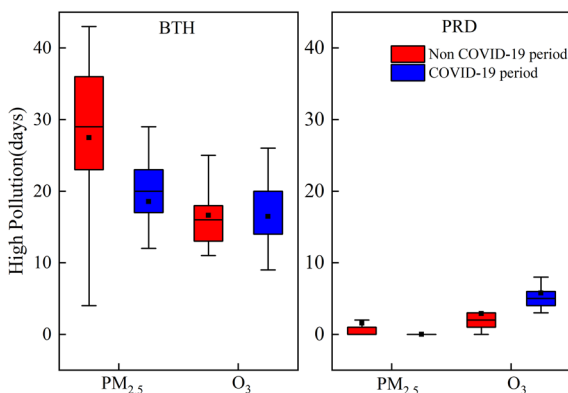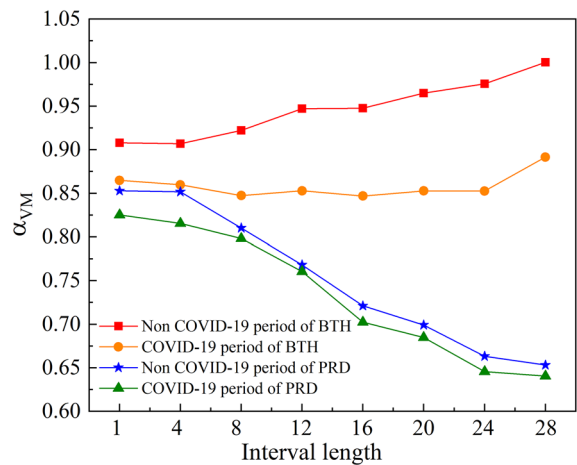

Fig. 8 Variations of average VM-DCCA exponents α_{VM} with interval length in BTH and PRD during the non-COVID-19 period and COVID-19 period

and 1.0 during the non-COVID-19 period, between 0.85 and 0.90 during the COVID-19 period, while those in PRD continuously decreases from 0.85 to 0.65 during the non-COVID-19 period, from 0.83 to 0.64 during the COVID-19 period. It reveals that with the increase of interval length, the long-term cross-correlation of the two high pollutants weakened in PRD, while remain stable in BTH.

Discussion

The SOC theory is used to explain the source of long-term persistence in the evolution of complex systems from a perspective of macro integrity. In the previous studies, Shi and Liu (2009) explained the scale invariant structures in the long-term evolution of PM$_{10}$, SO$_2$ and NO$_2$ in Shanghai based on SOC theory. Further, Shi et al. (2015) established a numerical sand pile model of pollutant evolution based on SOC theory to quantitatively explain the formation mechanism of stable long-term persistence of PM$_{2.5}$ during a typical haze period in Chengdu. Besides, Chelani (2016) pointed out that the emergence of long-term persistence in the temporal evolution of air pollution can be absolutely explained by SOC theory.

The evolution of the cross-correlation between high PM$_{2.5}$ and O$_3$ is highly similar to the known SOC system. Firstly, the atmosphere is an open dissipative system in which primary pollutants emitted

Fig. 7 Days of high pollution in BTH and PRD during the non-COVID-19 period and COVID-19 period

from human production and life provide material and energy. For example, primary pollutants NOx and VOCs generate $PM_{2.5}$ and O_3 through various atmospheric photochemical reaction pathways, a process analogous to the continuous input of sand grains into a sand pile. At the same time, some dissipative processes of these secondary pollutants through various pathways happen in atmospheric system. For example, high O_3 enhances atmospheric oxidation and promotes photochemical reactions, which rapidly depletes O_3. $PM_{2.5}$ pollutants can be transported on microscopic scales by diffusion or convection through rainfall deposition or wind diffusion, etc. This process is analogous to sand grains slipping in a sand pile. Secondly, pollutant components in the atmosphere can form short-range interactions through a variety of physical and chemical mechanisms. O_3 can influence the formation of NO_3^-, SO_4^{2-} and secondary aerosols by affecting the concentration of various oxidants. Correspondingly, $PM_{2.5}$ can affect O_3 formation directly or indirectly by influencing atmospheric dynamics, photolysis rates, cloud optical thickness and non-homogeneous reaction processes. This process is analogous to the mutual extrusion stress between sand grains. Thirdly, under stationary weather conditions, the interaction between $PM_{2.5}$ and O_3 will drive the entire atmospheric system to evolve spontaneously to a critical state and maintain it for a long time. Here, the short-term correlation between $PM_{2.5}$ and O_3 may cause a chain of forces involving the whole system, so as to evolve the long-term persistence. This process is analogous to the spontaneous evolution of a sand pile system to a SOC state due to the action of localised extrusion stresses between sand grains in a sand pile. Finally, in a critical state, the temporal correlation function of the atmospheric system to dissipation of external material or energy is power-law. The critical state of air pollution will continue to be locked as long as the external meteorological conditions of the stationary weather do not change, which is determined by the long-term persistent characteristics of the interaction between the pollution components ($PM_{2.5}$ and O_3) in the air pollution complex. This process is analogous to the power law distribution between the magnitude and frequency of sand pile collapse.

In Fig. 7, α_{VM} shows lower values during the COVID-19 period and varies with the interval length in BTH and PRD, which can be explained by the SOC

behavior. Driven by the input of primary and secondary pollutants, the cross-correlation of high $PM_{2.5}$ and O_3 experiences a stable internal dynamic process. In this case, external interference may destroy the short-term correlation between pollutants, thus affecting the long-term persistence of the cross-correlation between high $PM_{2.5}$ and O_3. At this time, critical state may be damaged and instability may occur. Regional meteorological factors and COVID-19 outbreak can be regarded as the external interference of atmospheric system. In general, higher temperature is accompanied by stronger solar radiation, resulting in stronger oxidation capacity and more active atmospheric photochemical reaction. In the PRD region, despite higher O_3 concentrations, the rapid depletion of O_3 itself and its precursors makes it difficult to maintain a lasting influence in the atmosphere. At the same time, higher RH and Pre may accelerate the coagulation and sedimentation of particulate matters, making it difficult for $PM_{2.5}$ to maintain a lasting impact in the atmosphere. The rapid consumption of high $PM_{2.5}$ and O_3 results in low α_{VM} values in PRD and decreases continuously with the increase of time scales. Besides, the increase of atmospheric oxidation capacity (AOC) caused by the rise of O_3 levels during COVID-19 may lead to low α_{VM} values. That is, the enhanced AOC accelerates the depletion of $PM_{2.5}$ and O_3 themselves and their precursors in atmospheric oxidation reactions, making it difficult to have lasting impacts in the atmosphere. Previous references have drawn some conclusions that can support this view. For example, Wang et al. (2020) found that the average O_3 concentrations increased by 20.1 $\mu g/m^3$ during the COVID-19 period in China. Huang et al. (2021) showed that the significant emission reduction of NOx during the COVID-19 promoted the increase of O_3 and the formation of HNO_3 free radicals at night, resulting in the increase of AOC. Qin et al. (2022) reported that the enhancement of AOC greatly affected $PM_{2.5}$ and O_3 and their relationship. Therefore, the long-term persistence of the cross-correlation between high $PM_{2.5}$ and O_3 during the COVID-19 period has weakened.

The greater the long-term persistence, the longer the cross-correlation between two pollutants. In this way, $PM_{2.5}$ (O_3) at a certain time will inevitably affect the formation of high O_3 ($PM_{2.5}$) at a certain time scale. This irresistible effect will increase the difficulty of coordinated control of $PM_{2.5}$-O_3 DHP in the future. The low α_{VM} values in PRD are conducive to

achieve the coordinated control of $PM_{2.5}$-O_3 DHP in some extent. Wu et al. (2021a) and Zhang et al. (2022) also found that $PM_{2.5}$-O_3 coordinated control is easier in Guangzhou, due to different meteorological factors, which is consistent with our results.

Therefore, the long-term persistence in $PM_{2.5}$-O_3 cross-correlation is closely related to the feasibility of coordinated control strategies. The relevant conclusions of this paper are helpful to the risk assessment and coordinated control of $PM_{2.5}$-O_3 DHP in different city clusters, which is of great significance in compound pollution prevention.

Conclusions

Based on the COVID-19 outbreak, this paper establishes a novel VM-DCCA model to study the long-term persistence of the cross-correlation between the high $PM_{2.5}$ and O_3 BTH and PRD.

The results show that the $PM_{2.5}$ levels are observed to have a decrease in most cities while the O_3 levels increased during the COVID-19 period, and the increase range of O_3 in the PRD (19.39%) is significantly greater than that in BTH (1.72%). Secondly, the DCCA results indicate that the cross-correlation between $PM_{2.5}$ and O_3 shows strong long-term persistence. The average DCCA exponents α of BTH is higher than PRD, and the non-COVID-19 period is higher than COVID-19 period. Finally, the VM-DCCA exponents α_{VM} between high $PM_{2.5}$ and O_3 during the COVID-19 period are generally higher than non-COVID-19 period, and BTH are higher than PRD. The average VM-DCCA exponents α_{VM} in PRD experience a significant downward trend with the increase of interval length, while remaining stable in BTH.

The above results showed that the spatiotemporal evolution of cross-correlation between high $PM_{2.5}$ and O_3 can be regarded as a typical SOC case. Based on the dynamic mechanism of SOC, the different response characteristics of $PM_{2.5}$ and O_3 pollutants in different regions during the COVID-19 period can be scientifically explained. The construction of VM-DCCA method related to high $PM_{2.5}$ and O_3 at different interval length is helpful to achieve coordinated control of pollutants.

Author contribution Bingyi Bao and Kai Shi analyzed the results and wrote the main manuscript text. Youping Li

prepared Figs. 1, 2, and 3, and Chunqiong Liu and Ye Wen prepared Figs. 4, 5, 6, 7, and 8. All authors reviewed the manuscript.

Data availability The data used to support the findings of this research are available from the corresponding author upon reasonable request.

Declarations

Ethics approval All authors have read, understood, and have complied as applicable with the statement on "Ethical responsibilities of Authors" as found in the Instructions for Authors and are aware that with minor exceptions, no changes can be made to authorship once the paper is submitted.

Conflict of interest The authors declare no competing interests.

References

Bak, P., Tang, C., & Wiesenfeld, K. (1987). Self-organized criticality: An explanation of the 1/f noise. *Physics Review Letters, 59*(4), 381–384.

Bherwani, H., Gautam, S., & Gupta, A. (2021). Qualitative and quantitative analyses of impact of COVID-19 on sustainable development goals (SDGs) in Indian subcontinent with a focus on air quality. *International Journal of Environmental Science and Technology., 18*(4), 1019–1028.

Chelani, A. (2016). Long-memory property in air pollutant concentrations. *Atmospheric Research, 171*(1), 1–4.

Chelani, A., & Gautam, S. (2022). Lockdown during COVID-19 pandemic: A case study from Indian cities shows insignificant effects on persistent property of urban air quality. *Geoscience Frontiers, 13*(6), 101284.

Chen, H. M., Zhuang, B. L., Liu, J., Wang, T. J., Li, S., Xie, M., Li, M. M., Chen, P. L., & Zhao, M. (2019a). Characteristics of ozone and particles in the near-surface atmosphere in the urban area of the Yangtze River Delta, China. *Atmospheric Chemistry and Physics, 19*(7), 4153–4175.

Chen, J. J., Shen, H. F., Li, T. W., Peng, X. L., Cheng, H. R., & Ma, C. Y. (2019b). Temporal and spatial features of the correlation between $PM_{2.5}$ and O_3 concentrations in China. *International Journal of Environmental Research and Public Health, 16*(23), 4824.

Chen, K., Zhou, L., Chen, X., Bi, J., & Kinney, P. L. (2017). Acute effect of ozone exposure on daily mortality in seven cities of Jiangsu province, China, No clear evidence for threshold. *Environmental Research, 155*, 235–241.

Chen, Y. Y., Cai, L. H., Wang, R. F., Song, Z. X., Deng, B., Wang, J., & Yu, H. T. (2018a). DCCA cross-correlation

coefficients reveals the change of both synchronization and oscillation in EEG of Alzheimer disease patients. *Physica A: Statistical Mechanics and Its Applications, 490*, 171–184.

Chen, L., Guo, B., Huang, J. S., He, J., Wang, H. F., Zhang, S. Y., & Chen, S. X. (2018b). Assessing air-quality in Beijing-Tianjin-Hebei region, The method and mixed tales of $PM_{2.5}$ and O_3. *Atmospheric Environment, 193*, 290–301.

Chen, Y. B., Wu, B., Zhang, J., Li, Y. H., & Shi, K. (2022). Impact of COVID-19 on chaotic evolution of O_3 in forest ecosystem. *Journal of China West Normal University (Natural Science), 43*(1), 9–17.

Chou, C. K., Tsai, C. Y., Chang, C. C., Lin, P. H., Liu, S. C., & Zhu, T. (2011). Photochemical production of ozone in Beijing during the 2008 Olympic Games. *Atmospheric Chemistry and Physics, 11*(6), 16553–16584.

Chu, B., Ma, Q., Liu, J., Ma, J., & He, H. (2020). Air pollutant correlations in China: Secondary air pollutant responses to NOx and SO_2 control. *Environmental Science and Technology, 7*, 695–700.

Ding, A. J., Fu, C. B., Yang, X. Q., Sun, J. N., Zheng, L. F., Xie, Y. N., Herrmann, E., Nie, W., Petäjä, T., Kerminen, V.-M., & Kulmala, M. (2013). Ozone and fine particle in the western Yangtze River Delta: An overview of 1 yr data at the SORPES station. *Atmospheric Chemistry and Physics, 13*(11), 5813–5830.

Du, J., Liu, C. Q., Wu, B., Zhang, J., Huang, Y., & Shi, K. (2021). Response of air quality to short-duration high-strength human tourism activities at a natural scenic spot: A case study in Zhangjiajie, China. *Environmental Monitoring and Assessment, 193*(11), 697.

Fu, X., Wang, T., Gao, J., Wang, P., Liu, Y. M., Wang, S. X., Zhao, B., & Xue, L. K. (2020). Persistent heavy winter nitrate pollution driven by increased photochemical oxidants in northern China. *Environmental Science and Technology, 54*(7), 3881–3889.

Gautam, S. (2020). COVID-19: Air pollution remains low as people stay at home. *Air Quality, Atmosphere & Health, 13*(7), 853–857.

Gautam, S., Samuel, C., Gautam, A. S., & Kumar, S. (2021). Strong link between coronavirus count and bad air: A case study of India. *Environment, Development and Sustainability, 23*(11), 16632–16645.

He, H. D. (2016). Multifractal analysis of interactive patterns between meteorological factors and pollutants in urban and rural areas. *Atmospheric Environment, 149*, 47–54.

Hu, M. M., Wang, Y. F., Wang, S., Jiao, M. Y., Huang, G. H., & Xia, B. C. (2021). Spatial-temporal heterogeneity of air pollution and its relationship with meteorological factors in the Pearl River Delta, China. *Atmospheric Environment, 254*(13), 118415.

Huang, X., Ding, A. J., Gao, J., Zheng, B., Zhou, D. R., Qi, X. M., Tang, R., Wang, J. P., Ren, C. H., Nie, W., Chi, X. G., Xu, Z., Chen, L. D., Li, Y. Y., Che, F., Pang, N. N., Wang, H. K., Tong, D., Qin, W., … He, K. (2021). Enhanced secondary pollution offset reduction of primary emissions during COVID-19 lockdown in China. *National Science Review, 8*(2), 51–59.

Jia, M. W., Zhao, T. L., Cheng, X. H., Gong, S. L., Zhang, X. Z., Tang, L. L., Liu, D. Y., Wu, X. H., Wang, L. M., & Chen, Y. S. (2017). Inverse relations of $PM_{2.5}$ and O_3 in air compound pollution between cold and hot seasons over an urban area of east China. *Atmosphere, 8*, 59.

Kumar, R. P., Perumpully, S. J., Samuel, C., & Gautam, S. (2023). Exposure and health: A progress update by evaluation and scientometric analysis. *Stochastic Environmental Research and Risk Assessment, 37*, 453–465.

Kumar, R. P., Samuel, C., Raju, S. R., & Gautam, S. (2022). Air pollution in five Indian megacities during the Christmas and New Year celebration amidst COVID-19 pandemic. *Stochastic Environmental Research and Risk Assessment, 36*, 3653–3683.

Le, T. H., Wang, Y., Liu, L., Yang, J. N., Yung, Y. L., Li, G. H., & Seinfeld, J. H. (2020). Unexpected air pollution with marked emission reductions during the COVID-19 outbreak in China. *Science, 369*(6504), 7431.

Li, W. G., Liu, X. G., Zhang, Y. H., Sun, K., Wu, Y. S., Xue, R., Zeng, L. M., Qu, Y., & An, J. L. (2018). Characteristics and formation mechanism of regional haze episodes in the Pearl River Delta of China. *Journal of Environmental Sciences, 63*(1), 236–249.

Liang, Y. Y., Liu, S. Y., & Zhang, S. L. (2017). Geary autocorrelation and DCCA coefficient: Application to predict apoptosis protein subcellular localization via PSSM. *Physica A: Statistical Mechanics and Its Applications, 467*, 296–306.

Liu, C. Q., & Shi, K. (2021). A review on methodology in O_3-NOx-VOC sensitivity study. *Environmental Pollution, 291*, 118249.

Liu, C. Q., Liang, J., Li, Y. P., & Shi, K. (2023). Fractal analysis of impact of $PM_{2.5}$ on surface O_3 sensitivity regime based on field observations. *Science of the Total Environment, 858*, 160136.

Liu, T., Wang, X. Y., Hu, J. L., Wang, Q., An, J. Y., Gong, K. J., Sun, J. J., Li, L., Qin, M. M., & Li, J. Y. (2020). Driving forces of changes in air quality during the COVID-19 lockdown period in the Yangtze River Delta region, China. *Environmental Science & Technology Letters, 7*(11), 779–786.

Muchnik, L., Bunde, A., & Havlin, S. (2009). Long term memory in extreme returns of financial time series. *Physica A: Statistical Mechanics and Its Applications, 388*(19), 4145–4150.

Peng, C. K., Havlin, S., Stanley, H. E., & Goldberger, A. L. (1995). Quantification of scaling exponents and crossover phenomena in nonstationary heartbeat time series. *Chaos, 5*(1), 82–87.

Piao, L., & Fu, Z. (2016). Quantifying distinct associations on different temporal scales: Comparison of DCCA and Pearson methods. *Scientific Reports, 6*, 36759.

Podobnik, B., & Stanley, H. E. (2008). Detrended cross-correlation analysis: A new method for analyzing two non-stationary time series. *Physical Review Letters, 100*(8), 084102.

Qin, M. M., Hu, A. Q., Mao, J. J., Zhang, Y. H., Hu, J. L., Li, X., Sheng, L., Sun, J. J., Li, J. Y., Wang, X. S., Zhang, Y. H., & Hu, J. L. (2022). $PM_{2.5}$ and O_3 relationships affected by the atmospheric oxidizing capacity in the Yangtze River Delta, China. *Science of the Total Environment, 810*, 152268.

Qin, Y., Li, J. Y., Gong, K. J., Wu, Z. J., Chen, M. D., Qin, M. M., Huang, L., & Hu, J. L. (2021). Double high pollution

events in the Yangtze River Delta from 2015 to 2019: Characteristics, trends, and meteorological situations. *Science of the Total Environment, 792*, 148349.

Qu, Y. W., Wang, T. J., Cai, Y. F., Wang, S. K., Chen, P. L., Li, S., Li, M. M., Yuan, C., Wang, J., & Xu, S. C. (2018). Influence of atmospheric particulate matter on ozone in Nanjing, China: Observational study and mechanistic analysis. *Advances in Atmospheric Sciences, 35*(11), 1381–1395.

Rohit, A., & Mitra, S. K. (2018). The co-movement of monetary policy and its time-varying nature: A DCCA approach. *Physica A: Statistical Mechanics and Its Applications, 492*, 1439–1448.

Shi, K. (2014). Detrended cross-correlation analysis of temperature, rainfall, PM 10 and ambient dioxins in Hong Kong. *Atmospheric Environment, 97*, 130–135.

Shi, K., & Liu, C. Q. (2009). Self-organized criticality of air pollution. *Atmospheric Environment, 43*(21), 3301–3304.

Shi, K., Liu, C. Q., & Huang, Y. (2015). Multifractal processes and self-organized criticality of $PM_{2.5}$ during a typical haze period in Chengdu, China. *Aerosol and Air Quality Research, 15*(3), 926–934.

Sun, T., Sun, R. H., Sadiq Khan, M., & Chen, L. D. (2021). Urbanization increased annual precipitation in temperate climate zone: A case in Beijing-Tianjin-Hebei region of North China. *Ecological Indicators, 126*, 107621.

Wang, Y. C., Yuan, Y., Wang, Q. Y., Liu, C. G., Zhi, Q., & Cao, J. J. (2020). Changes in air quality related to the control of coronavirus in China: Implications for traffic and industrial emissions. *Science of the Total Environment, 731*, 139133.

Wang, Y. S., Yao, L., Wang, L. L., Liu, Z. R., Ji, D. S., Tang, G. Q., Zhang, J. K., Sun, Y., Hu, B., & Xin, J. Y. (2014). Mechanism for the formation of the January 2013 heavy haze pollution episode over central and eastern China. *Science China, 57*(1), 14–25.

Wu, B., Liu, C. Q., Zhang, J., Du, J., & Shi, K. (2021a). The multifractal evaluation of $PM_{2.5}$-O_3 coordinated control capability in China. *Ecological Indicators, 129*, 107877.

Wu, J. S., Wang, Y., Liang, J. T., & Yao, F. (2021b). Exploring common factors influencing $PM_{2.5}$ and O_3 concentrations in the Pearl River Delta: Tradeoffs and synergies. *Environmental Pollution, 285*(1), 117138.

Xing, J., Wang, J. D., Mathur, R., Wang, S. X., Sarwar, G. L., Pleim, J., Hogrefe, C., Zhang, Y. Q., Jiang, J. K., Wong, D. C., & Hao, J. M. (2017). Impacts of aerosol direct effects on tropospheric ozone through changes in atmospheric dynamics and photolysis rates. *Atmospheric Chemistry and Physics, 17*(16), 9869–9883.

Xu, J., Zhang, Y. H., Zheng, S. Q., & He, Y. J. (2012). Aerosol effects on ozone concentrations in Beijing: A model sensitivity study. *Journal of Environmental Sciences, 24*(4), 645–656.

Yuan, N. M., & Fu, Z. T. (2014). Different spatial cross-correlation patterns of temperature records over China: A DCCA study on different time scales. *Physica A: Statistical Mechanics and Its Applications, 400*, 71–79.

Zhang, J., Li, Y. P., Liu, C. Q., Wu, B., & Shi, K. (2022). A study of cross-correlations between $PM_{2.5}$ and O_3 based on Copula and multifractal methods. *Physica A: Statistical Mechanics and Its Applications, 589*, 126651.

Zhao, H., Zheng, Y. F., & Li, C. (2018). Spatiotemporal distribution of $PM_{2.5}$ and O_3 and their interaction during the summer and winter seasons in Beijing, China. *Sustainability, 10*(12), 1–17.

Zhu, J., Chen, L., Liao, H., & Dang, R. (2019). Correlations between $PM_{2.5}$ and Ozone over China and associated underlying reasons. *Atmosphere, 10*(7), 352.